# The Interrelation of Local and Energy Criteria of Unstable Brittle Fracture for Low-Alloyed Cold Resistant Steels

Alexey Ilyin[1,a], Vladimir Filin[1]

[1] FSUE CRISM Prometey. 49, Shpalernaya str., St.-Petersburg, 191015, RUSSIA

[a] avctod@gmail.com, mail@crism.ru

**Keywords:** fracture toughness, unstable fracture, local and energy criterion, low-alloyed steel, size effect

**Abstract.** Experimental results evidence that some plastic work, even in case of cleavage fracture, is consumed by the propagating crack to reproduce a critical stress-strain state ahead its tip. This fact, contradicting to the "weakest link" simplification, should be taken into account in order to predict better the size, constraint and temperature effects correlating with the ratio of elastic and plastic parts of J-integral. Hence it is proposed to determine the condition of unstable brittle fracture in elastic-plastic materials based on the Griffith principle.

## Introduction

A local criteria approach [1,2] to the brittle fracture problem amplifies the traditional methods of linear-elastic (LEFM) or elastic-plastic (EPFM) fracture mechanics. The improvements concern the size effect and the effect of non-plane strain at the crack front on the fracture toughness examination, a particular behaviour of specimens with short cracks, etc. Generally, local criteria are employed when the correspondence of brittle fracture conditions to a critical value $J_c$ of J-integral becomes ambiguous. In terms of the local criteria approach, a failure of the weakest microstructural volume near a crack tip results in a macroscopic fracture of the whole specimen or structure. In other words, further propagation of a crack nucleated in the weakest microvolume consumes a negligibly low energy and there is no need to analyze such a process. On contrary, the Griffith principle suggests that the permanent reproduction of the critical stress-strain state (SSS) with no external work is essential for a brittle crack propagation.

An alternative explanation can be given by the authors [3] to the most experimental data, which had previously stimulated the "weakest link" theory development. The unstable failure condition is now considered as an energy balance between the rates of elastic strain energy release $G$ and plastic strain work $R$. From this point of view, failure of the weakest structural element near a crack tip is a necessary condition of brittle fracture, but there is also a sufficient condition formulated as an attainment of the critical SSS reproduced together with a propagating crack within some process zone. The local and energy fracture criteria prove to give the same predictions only for materials showing an elastic or nonlinear elastic behaviour. For a real elastic-plastic material this correspondence is also possible in case of small-scale plasticity (SSP) when the increment of a crack advance $\Delta a$ is close to the plastic strain zone size $r_{pl}$ ahead the crack tip. However, the latter condition means an extremely brittle state of the material.

The present study contains data supporting the energy criterion. These experimental results have been obtained for low-alloyed shipbuilding cold-resistant weldable steel in the grades F36...F690 with ferrite-bainite or predominantly bainite structure of the maximum grain size 10...20 μm. The chemical composition and mechanical properties of steel met the requirements of Russian Maritime Register of Shipping [4]. Actual impact energy values shown by Charpy specimens at the temperature down to -60°C were not less than 150 J. It should be noted that all the arguments for the

benefit of authors' proposals were obtained on steel of the same type, so the authors admit their possible restrictions.

**1. Unstable Fracture Energy Criterion Formulation for an Elastic-Plastic Material**

The energy balance for crack propagation with no work of external forces and no significant contribution of kinetic energy may be written as follows [5]:

$$G = R + C, \tag{1}$$

where

$$G = -\lim_{\Delta a \to 0} \frac{1}{\Delta a} \int_V \Delta w_{\text{el}} dV, \tag{2}$$

$$R = \lim_{\Delta a \to 0} \frac{1}{\Delta a} \int_{V_{\text{pl}}} \Delta w_{\text{pl}} dV_{\text{pl}}, \tag{3}$$

$\Delta w_{\text{el}}$, $\Delta w_{\text{pl}}$, are increments of the elastic strain energy and plastic strain work densities;
$\Delta a$ is an increment of a crack advance;
$V$, $V_{\text{pl}}$ are the total volume and the volume of a plastic deformation zone;
$C$ is a work spent to produce a new crack surface unit, for type I crack it is determined as

$$C = \lim_{\Delta a \to 0} \frac{1}{\Delta a} \int_{\Delta a} \left( \int \sigma_1 du_1 \right) dx, \tag{4}$$

where $\sigma_1$ is the principal stress perpendicular to the fracture surface and acting just before the crack advance;
$u_1$ is the crack opening displacement realized after the crack advance.

If we suppose that cleavage triggering sites are located in the zone of maximum principal stress and $\Delta a \sim (2\ldots3)\delta$, where $\delta$ is a crack tip opening displacement (CTOD), then $\Delta a / r_{\text{pl}} = (2...3)\sigma_{\text{Y}}/E$, i.e., $\Delta a << r_{\text{pl}}$. Here $\sigma_{\text{Y}}$ is a yield stress, $E$ is a modulus of elasticity. In this case $C << R$ and $C \to 0$ at $\Delta a \to 0$ [6]. Therefore, for an elastic-plastic material

$$G = R. \tag{5}$$

For linear- or nonlinear-elastic materials the opposite case takes place: $R = 0$ and $G = C$.
In order to analyze the interrelation of $G$ and $J$-integral it should be noted that the equality $G = J$ is not met for elastic-plastic materials. This is the most evident for loads corresponding to the full-scale plasticity (FSP), when $G$ is obviously limited by the elastic part of $J$-integral ($J_{\text{el}}$). For loads corresponding to the small-scale plasticity (SSP) it is less evident but can be illustrated by Figure 1.
Figure 1,*a* presents load vs. displacement curves for two specimens made of a nonlinear elastic material with crack lengths $a$ and $(a + \Delta a)$. A small-scale nonlinear area corresponding to the SSP zone of a real material can be seen in this diagram if its scale allows to distinguish the difference in specimens' compliances. After a crack advance ($\Delta a$) the SSS near the crack tip reproduces to the same distance $\Delta a$, and the area *OABO* is equal to $G \cdot \Delta a$. Figure 1,*b* shows the same curves for an elastic-plastic material. Here the non-hatched part of the area *OABO* corresponds to some plastic work spent to shift the nonlinearity area ($R$). The increment of elastic strain energy $G$ may be defined as a difference between the energies of specimens with crack lengths $a$ and $a + \Delta a$ but the same (non-reproduced) SSS.

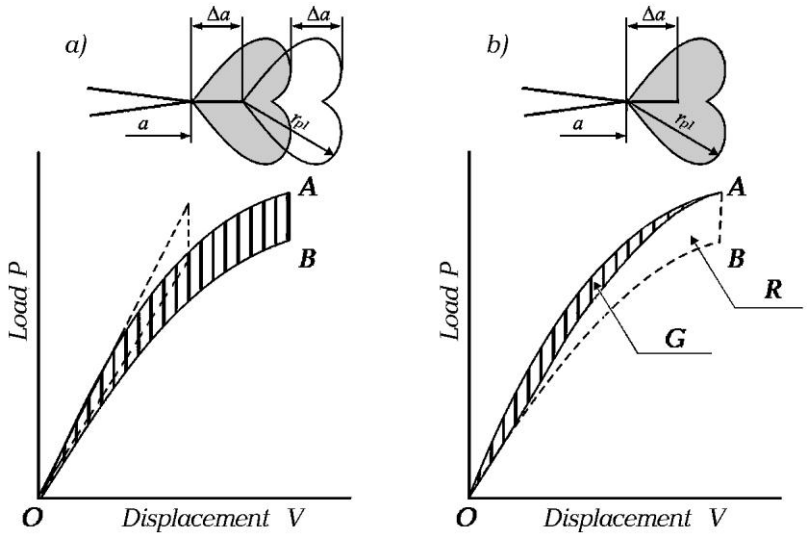


Fig 1. Definition of $G$ (hatched areas) for nonlinear elastic (*a*) and elastic-plastic (*b*) materials (in assumption that $\Delta a < r_{pl}$).

J-integral equation for a non-linear elastic material with no work of external forces may be written as

$$J = -\partial\Pi/\partial a = -\left[\iint_V \partial w_{el}^*/\partial a \, dx\, dy + \iint_V \partial w_{pl}^*/\partial a \, dx\, dy\right], \quad (6)$$

where $w_{el}^*$, $w_{pl}^*$ are linear and nonlinear parts of strain energy density respectively, and $\Pi$ is a potential energy.

For an elastic-plastic material the first component in (6) is $G$, the second one is $R$ because $w_{pl}^* = -w_{pl}$ for reproduced SSS in SSP conditions. Consequently, $J = G + R$, and, with (5) taken in mind, it follows that

$$G = J/2. \quad (7)$$

In FSP conditions $J >> J_{el}$, and a crack advance causes a decrease of the ultimate load $P$. The following example may be given for a SENB-type specimen:
— load decrease

$$dP/da = 2P/(W-a), \quad (8)$$

where $W$ is a specimen width,

— compliance change (approximation applied)

$$d\lambda/da = 2\lambda/(W-a), \quad (9)$$

where $\lambda$ is a specimen compliance,

— rate of elastic strain energy release

$$G = \lambda P^2/(W-a) = \frac{P^2}{2}\cdot\frac{d\lambda}{da}, \quad (10)$$

where the right part of the equality presents the well known formula for $J_{el}$. Hereby in conditions of FSP and $J >> J_{el}$ the value of $G$ can be determined as

$$G = J_{el}. \quad (11)$$

The following formula is proposed to make interpolation between (7) and (11) for intermediate cases when $J$ is defined as a sum of plastic $J_{pl}$ and elastic $J_{el}$ parts:

$$G = \frac{J_{el}}{1 + J_{el} / J}. \qquad (12)$$

An acceptability of (12) has been confirmed by a series of FEM calculations performed on a half SENB specimen model with a crack located along the symmetry plane [3]. The model was preloaded with further displacement prohibition of the load point. The crack advance was simulated in the way of node-by-node release from the symmetry plane. The values of $J$ и $J_{el}$ at crack start, mesh size and crack advance step were varied. After some steps the reproduced SSS became steady. The values of $G$ and $R$ were found by summation of elastic energy and plastic work increments in the whole volume of simulated specimen. Figure 2 presents the examples of numerical results.

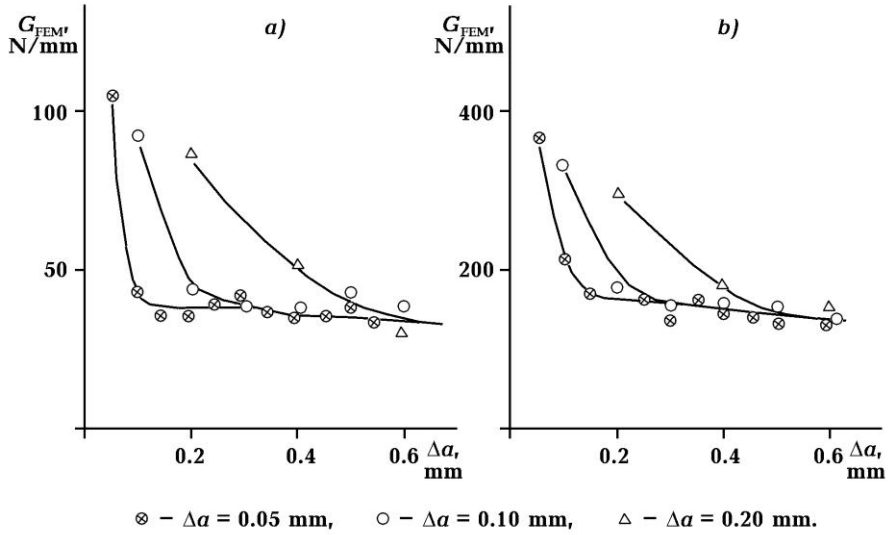


Fig. 2. Values of $G$ calculated at FEM simulation of a crack advance in SENB specimens.
*a*) $J$ = 91 N/mm, $J_{el}$ = 82 N/mm, *b*) $J$ = 690 N/mm, $J_{el}$ = 208 N/mm.

In terms of the proposed approach, the unstable brittle fracture condition is formulated as

$$G \geq R. \qquad (13)$$

For SSP loads it is equal to the commonly used criterion $J \geq J_c = \text{const}$. But for FSP loads the critical $J$ depends on $J_{el}/J$ ratio that is governed by specimen geometry. When $R > J_{el}$, the brittle fracture is impossible at all.

**2. Results of metallographic examination**

Figure 3 shows some metallographic examination results for 40 mm thick SENB specimens made of steel F690. Fracture toughness tests have been performed at different temperatures $T$, at $T$ = -40°C critical CTOD values $\delta_c$ = 0.18…0.25 mm. Several specimens were unloaded before rupture and cut at their mid-thickness across the crack front to make micro sections.

Cleavage-type damage traces have been observed ahead of the crack blunting. Their length depends on attained CTOD values, Fig.3: 6 μm for δ = 0.025 mm, 15μm for δ = 0.08 mm, 160 μm for δ = 0.15 mm. This way, the damage process ahead a crack tip seems more complicated if cleavage nucleates but the energy criterion is not met, in this case cleavage traces are integrated into the

advanced crack and slip-mode fracture is observed (Fig. 3,*c*). This case clearly discerns from the picture of a stable ductile crack growth at $T$ = +20°C shown in Fig. 3,*d*.

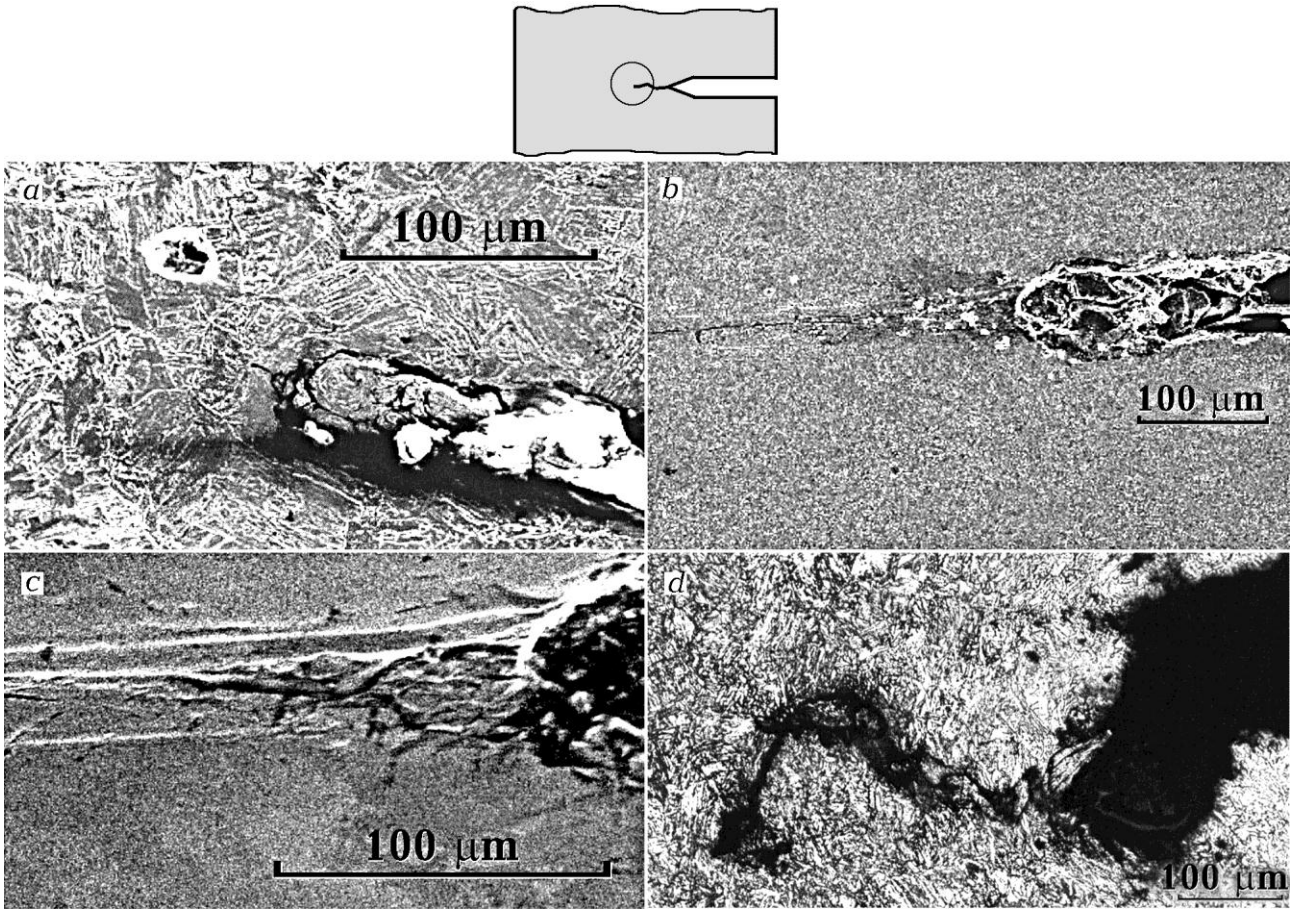


Fig. 3. Damage process near the crack tip at -40°C (*a* – *c*) and +20°C (*d*). Crack tip opening δ measured under the maximum test load amounts to 0.08 mm (*a*), 0.15 mm (*b*, *c*) and 0.80 mm (*d*).

**3. Results of X-ray diffraction examination**

The main supposal of the present study is the necessity of some plastic work to realize an advance of unstable brittle fracture. X-ray diffraction analysis of fracture surfaces has been applied as a rough method to evaluate the order of magnitude of this work. This method allows to estimate the strain distribution in the direction of depth in the way of measuring the diffraction line half-width β during step-by-step electrolyte etching of a crystalline type fracture surface [7]. This examination has been carried out for fracture surfaces of SENB fracture toughness specimens made of steel F620 tested at different temperatures. Table 1 presents some obtained data.

Reference pretests had been undertaken to obtain the dependence of β vs. plastic strain $e_{\text{pl}}$. The Cr-Kα emission, and diffraction line from (211) crystalline planes were used. For shipbuilding weldable steels considered in this study the following empirical equation was obtained:

$$\beta/\beta_0 = 1 + 3.5e_{\text{pl}}, \tag{14}$$

where $\beta_0$ is a value of β for annealed steel.

The value of $R$ is these examinations was assessed as

$$R_{\text{X-ray}} = 2\int_0^h \sigma_{\text{Y}} e_{\text{pl}}(y)dy \ , \tag{15}$$

where $e_{pl}(y)$ is a strain distribution in the depth direction,
$h$ is a depth of the deformed layer.

Table 1. Fracture toughness and X-ray examination results

| Fracture toughness test temperature, °C | $J_c$ for unstable failure, N/mm | $J_{el}$ for unstable failure, N/mm | $R$, N/mm (5, 12) | $R_{X\text{-}ray}$, N/mm (15) |
|---|---|---|---|---|
| -20 | 450 | 75 | 64 | 50 |
| -60 | 220 | 72 | 54 | 34 |
| -80 | 40 | 40 | 20 | 10 |

Data of Table 1 lead to the following conclusions.
i) $R_{X\text{-}ray}$ increases as the temperature elevates (even though there are no visually detected changes in the crystalline type of fracture).
ii) $R_{X\text{-}ray}$ is closer to the calculated $R$ (or $J_{el}$) than to $J_c$ corresponding to the crack start, and, at least, it appears comparable with $J_{el}$ but never close to zero.

**4. Size and constraint effects and their interpretation based on the proposed energy criterion**
As it is shown above, unstable brittle fracture occurs if

$$\frac{J_{el}}{1+J_{el}/J} = \text{const}, \tag{16}$$

so its condition is two-parametric for tests with nonlinear load-displacement diagrams. It means that the fracture toughness parameters measured in tests depend on specimen type and dimensions. Specimens of each type and size exhibit their own dependences $J_{el}(J)$. If strain hardening of material is omitted, this dependence may be expressed as follows:

$$J_{el} = J_Y\left[1-(q^2n^2-1)\left(\frac{J-J_Y}{J}\right)^2\right], \tag{17}$$

where $J_Y$ is a value of $J$ calculated from the simplest beam theory and corresponding to the yield stress attainment in the specimen ligament;
$q$ is a factor considering the increase of bending moment up to the ultimate value for a bent beam, $q$ = 1.5 for a SENB specimen;
$n$ is a factor considering the constraint effect, its maximum value is 1.4 if Mises theory is applied to a plain-strain loaded SENB specimen.

The empirical equation (17) is well confirmed by experimental data. It allows to describe the size effect and the constraint effect from the proposed point of view.
For SENB specimens with a crack length $a \approx W/2$ prescribed by standards, $J_Y$ can be found as

$$J_Y = 0.395\sigma_Y^2(W-a)/E. \tag{18}$$

Hence the $J_{el}/J$ ratio decreases and $J_c$ increases for specimens of smaller size. This effect is related to the lowering ligament size ($W - a$) but not to the decreasing crack front length equal to specimen thickness $B$ as it is expected in terms of the local criteria approach. The next prediction from the present study says that the lowest size effect will be observed if both large and small specimens fail at SSP loads, and the highest one when the smaller specimen does not exhibit brittle fracture due to the restricted maximum $J_{el} < R$.

Since the commonly used specimens have a rectangular section with the dimensions $(W - a) \approx B$ where $B$ is close to the full thickness of investigated material, both approaches lead to similar predictions. So an experiment has been undertaken with specimens of the different ratio $(W - a)/B$ and thickness. Table 2 presents the test results. Two series of B×B specimens were tested to verify the homogeneity of material in respect of fracture toughness in different directions.

Table 2. Test results for specimens made of steel F36 with various net section dimensions

| Specimen designation | Thickness $B$, mm | Width $W$, mm | Ligament size $(W - a)$, mm | Average $J_c$, N/mm | Fracture plane identification |
|---|---|---|---|---|---|
| B×2B | 40 | 80 | 40 | 250 | Y-X |
| B×B | 40 | 40 | 20 | 410 | Y-X |
| B×B | 40 | 40 | 20 | 420 | Y-Z |
| 2B×B | 80 | 40 | 20 | 420 | Y-Z |
| 1/2B×B | 20 | 40 | 20 | 610 | Y-X |

As predicted by the weakest link theory, fracture toughness parameters will increase in the following order: 2B×B, B×2B, B×B (the series B×2B and B×B would show the same result), 1/2B×B. An alternative sequence based on the energy approach is B×2B, 2B×B, B×B, 1/2B×B. For the latter three series the ligament size is the same but the factor $n$ in (17) depending on the ratio $(W - a)/B$ sequentially decreases. The results given in Table 2 testify to the energy criterion.

Another difference in size effect prediction by both approaches may be found while analyzing the data shown in Fig. 4. Here the fracture toughness results obtained with SENB specimens of 37 mm and 10 mm in thickness made of F420 steel are compared. Axis X gives $J_c$, axis Y represents the corresponding $J_{el}$. The test temperature (-100°C) corresponds to the case when a part of small specimens cannot exhibit brittle fracture (those results are not shown here), hence the highest size effect for two series should be observed.

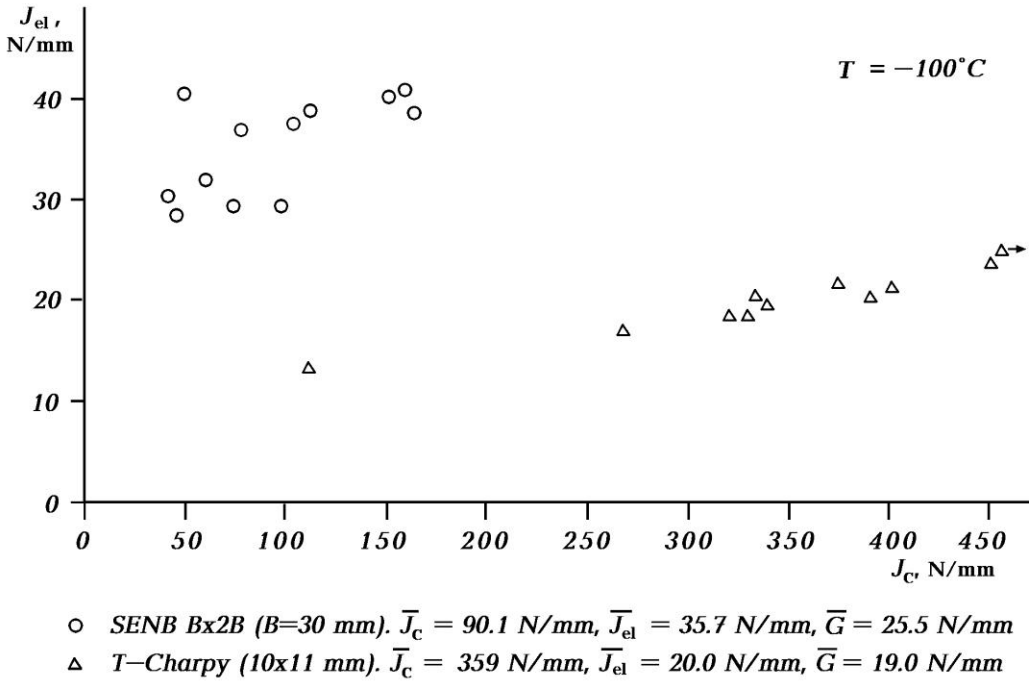


Fig.4. Interrelation of $J_{el}$ and critical $J$ for SENB specimens of different thickness, and results of $G$ calculation

Based on the local criteria approach, the predicted critical $J$ ratio for small and large specimens should be about 1.9. In fact this ratio is equal to 4. The values of $G$ calculated from (12) are just the same for both series that testifies to the energy approach.
The "constrained effect" can be described here as a dependence of factors $n$ and $q$ from the type of loading ($n$ and $q$ for tensed CCT specimens are lower than for bent SENB and CT ones), and specimen dimensions, i.e. ratios $(W-a)/B$ and $a/W$. In terms of the local criteria approach this effect is explained as a reduction of the maximum principal stress level in a process zone when loading conditions deviate from plain strain. This explanation is open to argument because there is no essential reduction of stress level directly in cleavage nucleation sites within the crack blunting area. The proposed approach allows to understand how the changes of SSS distant from the most likely cleavage triggering sites effect on the brittle fracture conditions.

**Conclusion**

Unlike the local criteria approach to the brittle fracture problem, the energy approach suggests the cleavage condition for a mesoscopic volume combined of many microstructural elements. This seems to provide a better explanation of the $J_c$ temperature dependences; in particular, the fact that actual values of $J_c$ at the "upper" shelf are 30...40 times higher than at the "lower" shelf. Indeed, with the simplest fracture criterion, the probability $p$ of cleavage in a microstructural element is

$$p(\sigma) = \left( \frac{\sigma_1}{\sigma_u} \right)^m , \qquad (19)$$

where $\sigma_u$ and $m$ are temperature-independent constants of the material.

An actual variation in yield strength within the ductile to brittle transition temperature interval could solely correspond with the above mentioned range of $J_c$ at factor $m$ not less than 20...30. The latter would be unrealistic for any parameter related to the microstructure. At the same time, if the brittle fracture is supposed to be a simultaneous realization of independent cleavage events in a number of microstructural elements, then $m$ becomes high as a sum of exponents related to numerous events. This suggestion also explains why fracture toughness is well correlated with average structural parameters but not with any "tails" of their distributions.

**References**


[1] Beremin F.M et. al. A local criterion for cleavage fracture of nuclear pressure vessel steel. Metal Transactions A. Vol. 14, Issue 11 -1983. - p. 2277-2287.

[2] J. Hohe, J. Wenck, D. Siegele. Assessment of the role of micro defect nucleation in probabilistic modeling of cleavage fracture. *EUROMECH - MECAMAT 2006*. J. Besson, Ed. MINES Paris, 2006. - p. 21-26.

[3] Ilyin A.V., Mizetsky A.V., Filin V.Yu. Regarding scale effect during tests for cracking resistance using modified Griffith approach.— Problems of Material Science, 2005, N 1 (41), p. 55-69 (in Russian).

[4] Rules for Classification and Construction of Sea-going Ships. Russian Maritime Register of Shipping. Vol. II, Edition XV, 2012. - 639p.

[5] K. Hellan. Introduction to Fracture Mechanics. McGraw-Hill, New York, 1984. - 302p.

[6] Kfouri A.P., Rice, J.R. Elastic-plastic separation energy rate for crack advance in finite growth steps. *Fracture 1977*, Vol. 1, D.M.R. Taplin, Ed. University of Waterloo Press, Ont., 1978, p. 43.

[7] Klevtsov G.V., Botvina L.R., Gorbatenko N.A. X-ray methods of fracture diagnostics in metallic materials. Russian Journal of Nondestructive Testing, N 4, 1994.- p. 86-98 (in Russian).